DOI: 10.1002/ejic.200600559

"Pincer" N-Heterocyclic Carbene Complexes of Rhodium Functionalised with Pyridyl and Bipyridyl Donors

Joseph A. Wright,[a] Andreas A. Danopoulos,*[a] William B. Motherwell,*[b] Robert J. Carroll,[b] Simon Ellwood,[c] and Jörg Saßmannshausen[d]

Keywords: Rhodium / Carbene ligands / Tridentate ligands / N ligands / Ligand design

The "pincer"-type carbene complexes Rh(C–N–C)Cl and Rh(C–N–N)Cl [C–N–C = 3,3′-diaryl-1,1′-pyridine-2,6-diylbis-(imidazol-2-ylidene), C–N–N = 1-aryl-3-(2,2′-bipyridin-6-yl)-imidazol-2-ylidene] have been prepared and characterised by spectroscopic and diffraction methods. They bind CO to give cationic complexes but are inert to H_2. Both oxidatively add CH_2Cl_2 to give octahedral Rh^{III} complexes. Theoretical calculations provide insight into the bonding of the Rh(C–N–C)Cl and Rh(C–N–N)Cl complexes.

Introduction

Since the development of the first route to free N-heterocyclic carbenes (NHCs),[1] ligands based around the stabilised-carbene core have become a major focus of research activity. Interest in N-heterocyclic carbene (NHC) metal complexes is now expanding to the study of new versatile ligand topologies with "classical" functional groups, which have shown promising spectator characteristics.[2] One of these is the "pincer" architecture, which provides a preorganised backbone capable of blocking meridional or pseudo-meridional coordination sites of the metal atom, leaving the remaining available for catalysis.[3] "Pincer" phosphane, amine, amide, imine, thioether and oxazoline complexes have been extensively studied and show very useful properties,[4] for example, unusually high thermal and air stability, stabilisation of uncommon oxidation states, stabilisation of unstable fragments on the metal atom, helical chirality and catalytic activity.

As part of our ongoing studies involving the use of the versatile "pincer" ligand 3,3′-diaryl-1,1′-pyridine-2,6-diylbis(imidazol-2-ylidene) (C–N–C),[5] we now report the formation and reactivity of rhodium(I) and rhodium(III) species based on this ligand system. We also detail the synthesis of a novel bipyridylcarbene ligand (C–N–N) and the formation of the derived rhodium complexes.

Results and Discussion

(C–N–C)Rh^{I} and -Rh^{III} Complexes

Interaction of the free carbene **1** with $[Rh(alkene)_2Cl]_2$ (alkene = ethene, cyclooctene) in THF at either room temperature or –78 °C gave a rapid colour change from orange to deep purple (Scheme 1).

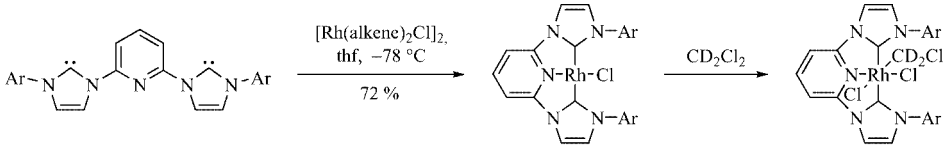

Scheme 1. Synthesis of rhodium complexes **2** and **3** (alkene = C_2H_4, C_8H_{14}; Ar = 2,6-*i*$Pr_2C_6H_3$).

Following removal of the solvent, a deep purple microcrystalline solid was obtained, which was sparingly soluble in benzene but readily re-dissolved in THF. The planar symmetry of the complex was supported by NMR spectroscopy. The proton spectrum in [D_8]THF showed two doublets at δ = 1.15 and 1.44 ppm (12 H each), along with a single septet at δ = 3.06 ppm (4 H), supporting the pres-

[a] School of Chemistry, University of Southampton, Highfield, Southampton, SO17 1BJ, UK
[b] Christopher Ingold Laboratories, University College London, 20 Gordon Street, London, WC1H 0AJ, UK
[c] Quest International, Kennington Road, Ashford, Kent, TN24 0LT, UK
[d] TU Graz, Institute for Chemistry and Technology of Organic Materials, Stremayrgasse 16/I, 8010 Graz, Austria
E-mail: ad1@soton.ac.uk

Supporting information for this article is available on the WWW under http://www.eurjic.org or from the author.

ence of equivalent isopropyl groups on the bulky DiPP [2,6-(diisopropyl)phenyl] groups. The $^{13}C\{^1H\}$ NMR spectrum also is in agreement with a symmetric structure; however, the C_{NHC} signal was not observed. Crystals of **2** suitable for X-ray diffraction were grown by slow diffusion of petroleum ether into a THF solution of the complex (Figure 1).

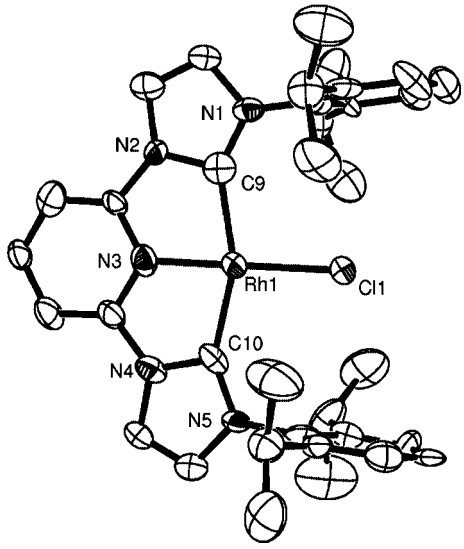

Figure 1. ORTEP representation of the structure of **2** showing 50% probability ellipsoids with hydrogen atoms omitted for clarity. Selected bond lengths [Å] and angles [°] with estimated standard deviations: Rh(1)–Cl(1) 2.331(3), Rh(1)–N(3) 1.955(8), Rh(1)–C(9) 2.001(10), Rh(1)–C(10) 1.979(9); N(3)–Rh(1)–Cl(1) 178.4(3), N(3)–Rh(1)–C(9) 78.5(4), N(3)–Rh(1)–C(10) 79.4(4), C(9)–Rh(1)–Cl(1) 101.2(3), C(10)–Rh(1)–Cl(1) 100.8(3).

The coordination sphere around the metal atom is essentially square-planar. The rhodium centre lies 0.027(4) Å out of the mean plane defined by the coordinating atoms. The Rh–C_{NHC} bond lengths [2.001(10) and 1.979(9) Å] are typical for rhodium(I)–C_{NHC} bond lengths. Complex **2** constitutes the first structurally characterised dicarbene complex of Rh^I in which the coordination sphere is comprised of non-π-acidic ligands. The synthesis of the analogous [(C–N–C)Rh(CO)](PF_6), where C–N–C = 3,3′-dialkyl-1,1′-pridine-2,6-diylbis(imidazol-2-ylidene) (alkyl = methyl, ethyl, benzyl) has been recently reported, together with reactivity studies towards the oxidative addition of methyl iodide.[6] In addition, (C–N–C)$RhBr_3$ has been prepared by reaction of the corresponding imidazolium salt with $[Rh(COD)Cl]_2$ and triethylamine in acetonitrile.[7]

Dissolution of complex **2** in CD_2Cl_2 initially gave a purple solution, which became yellow within a few minutes. The NMR spectra of this solution showed a lowering of the molecular symmetry of the new complex compared to **2**. It comprised two signals for the methine groups (integrating for 2 H each), along with four signals for the methyl groups of the *i*Pr groups (each integrating for 6 H). However, the signals assigned to the pyridine and imidazol-2-ylidene backbones retained the same appearance as in the starting material. These changes are in line with oxidative addition to the metal centre and consistent with the structure proposed for **3** in Scheme 1. On standing, crystals of **3** formed from the CD_2Cl_2 solution, and these were suitable for a single-crystal diffraction study (Figure 2).

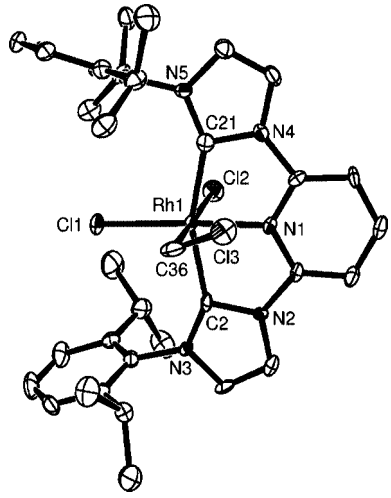

Figure 2. ORTEP representation of the structure of **3** showing 50% probability ellipsoids with hydrogen atoms and one molecule of CD_2Cl_2 omitted for clarity. Selected bond lengths [Å] and angles [°] with estimated standard deviations: Rh(1)–Cl(1) 2.3656(15), Rh(1)–Cl(2) 2.5164(16), Rh(1)–C(36) 2.075(6), Rh(1)–N(1) 1.978(4), Rh(1)–C(21) 2.034(6), Rh(1)–C(2) 2.040(6); N(1)–Rh(1)–Cl(1) 177.68(15), N(1)–Rh(1)–C(21) 79.1(2), N(1)–Rh(1)–C(2) 79.2(2), C(36)–Rh(1)–Cl(2) 177.22(19).

Complex **3** adopts an unsymmetrical distorted octahedral geometry, with the tridentate "pincer" occupying meridional sites with the remaining sites being occupied by two *cis*-chlorine atoms and the CH_2Cl group. The Rh–C_{NHC} bond lengths in complexes **2** and **3** are the same within the observed esds [averages of 1.990(13) and 2.037(8) Å, respectively]. However, the rhodium–chloride distances for the chloride ion bound *trans* to $N_{pyridine}$ are significantly different: the Rh–$N_{pyridine}$ bond in **3** [2.3656(15) Å] is longer than that in **2** [2.331(3) Å]. This is presumably due to the more crowded environment around the metal atom in the octahedral complex **3**. The two Rh–Cl distances in **3** are also significantly different from each other: the Cl ion *trans* to the CD_2Cl group is approximately 0.15 Å further from the Rh atom than that *trans* to the $N_{pyridine}$ atom.

Complex **2** showed oxidative reactivity with a range of alkyl halides and pseudohalides. For example, addition of methyl iodide, 1,1,1-trichloroethane, benzyl chloride or methyl triflate to **2** in THF led to colour changes from purple to light yellow. The time taken for these reactions varied from seconds (CH_3I) to overnight (1,1,1-trichloroethane), presumably due to the differing reactivity of the C–halide bond. The NMR spectra of all products demonstrated the same lowering of symmetry as seen in **3**, although additional changes were also seen which could not be readily assigned. Addition of phosgene to **2** also gave a rapid and clean oxidative addition, leading to a stable unsymmetrical product. Complex **2** also reacted very fast with oxygen both in solution and in the solid state; the organometallic product from the oxidation has not been characterised.

In contrast to the rapid reactions observed with alkyl halides and oxygen, complex **2** was unreactive towards other potential reagents for oxidative addition. No reaction was observed with triethylsilane, phenyldiazomethane or PhS=CHPh.[4e] In all cases, ^{1}H NMR spectra indicated that the starting material was unchanged. Similarly, no reactivity was seen with benzene (heating solutions of the complex in C_6D_6 in a sealed system to over 150 °C or exposure of the solution to UV light). Attempts to derivatise **2** by substitution of the chloride ion with organolithium compounds and Grignard reagents under various conditions were likewise unsuccessful.

Reactivity with CO

Hydroformylation is a major industrial process, and (phosphane)rhodium complexes are widely used for the formation of short-chain (C_2 to C_5) aldehydes under these conditions.[8] However, some phosphane complexes are unsuitable for use with other substrates due to thermal degradation. The development of novel rhodium-based hydroformylation catalysts for heavier alkenes (C_8 and higher) remains a challenge. As a probe for potential hydroformylation activity, the reactivity of **2** towards synthesis gas and carbon monoxide was studied (Scheme 2).

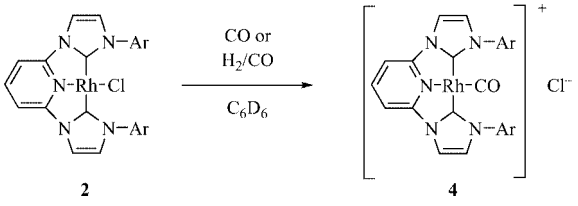

2 **4**

Scheme 2. Reaction of complex **2** with CO (Ar = 2,6-*i*Pr$_2$C$_6$H$_3$).

Bubbling a mixture of H_2/CO (1:1) through a C_6D_6 solution of **3** resulted in a fast irreversible colour change from purple to pink. Evaporation of the solvent from the mixture gave a light pink, air-stable complex **4** which is noticeably more soluble in C_6D_6 than the parent complex. ^{1}H NMR spectra indicate that the products obtained with CO and CO/H_2 are identical; as a confirmation of this, no reaction was observed with hydrogen gas alone. The ^{1}H or ^{13}C{^{1}H} NMR spectra of **4** show the same symmetry to **2**. However, in the ^{1}H NMR spectrum, a significant change occurs in the shift of one of the imidazole backbone signals (from δ = 8.15 ppm to δ = 10.42 ppm on coordination of CO). The electrospray mass spectrum of **4** shows a single signal at *m*/*z* = 662.5, consistent with an adduct of the (pincer)rhodium core and CO. Complex **4** also shows only a single IR stretch at 1968 cm^{-1}. This compares with 1982 cm^{-1} reported for [Rh(C–N–C)(CO)](PF$_6$) and 1980 cm^{-1} for [Rh(P–N–P)(CO)]Cl {P–N–P = 2,6-bis[(diphenylphosphanyl)methyl]-pyridine}.[6,9] Attempts to grow single crystals of **4** were unsuccessful, and anion exchange also failed to give useful products.

Whilst the reactivity of **4** with carbon monoxide was rapid, the high stability of the product indicated possible problems in hydroformylation. NMR-scale addition of ethene to **2** showed no reaction. The hydroformylation activity was investigated using synthesis gas and styrene. No reaction was observed under a range of conditions, and a pink-coloured solution was recovered. Thus, it seems likely that under hydroformylation conditions an irreversible coordination of CO occurs to give **4**, whilst **2** will not bind alkenes or hydrogen.

Bipyridyl NHC Ligands

Even though the C–N–C ligand **1** is considered a strong σ-donor, its limitations became apparent from the inactivity of **2** in hydroformylation which could be ascribed to the low lability of the Rh–C_{NHC} bond hindering the formation of coordinatively unsaturated catalytic sites. In addition, due to the strong σ-donating ability of the NHC donors, **1** may be better suited for the stabilisation of Rh^{III} rather than the promotion of Rh^{I}–Rh^{III} catalytic cycles. Therefore, we decided to explore the chemistry of alternative "pincer" ligand designs by replacing one of the NHC donors of the C–N–C system with another classical donor. Whilst there is clearly a large range of potential ligands which could be constructed around this motif, we have concentrated on an NHC–bipyridyl system **7** (Scheme 4). Recently, Milstein has reported nonsymmetrical pincer-type ligands bearing phosphane and amine wingtips.[10]

The necessary bromide **4** is available in three steps from commercially available 2,2′-bipyridine.[11,12] Quaternisation of **4** with the imidazole **5** (Scheme 3) proceeds smoothly in the melt at 160 °C, giving moderate yields of the desired imidazolium bromide after purification and azeotropic drying. In contrast to the pincer imidazolium salts of the C–N–C type, deprotonation of **6** could not be readily achieved under the standard conditions[5a] which involved the reaction with KN(SiMe$_3$)$_2$ in THF at –30 °C, followed by addition of toluene (to precipitate the KBr formed in the reaction). This method gave only low yields of **7** (less than 5%). As an alternative to deprotonation, we explored the reductive deprotonation of the imidazolium salt with potassium metal, which has recently been used for the preparation of IMes from (IMesH)$^+$Cl$^-$.[13] This methodology, when applied to the preparation of **7**, resulted in improved isolated yields (ca. 30%) allowing the study of the coordination chemistry of **7**. The structure of **7** was also determined crystallographically (Figure 3).

In common with other free-carbene solid-state structures,[14] the free-carbene and pyridine rings adopt a *trans* arrangement. The three donor-atom-containing rings are virtually coplanar, with interplane angles of 3.3(2)° (carbene–pyridine) and 2.7(2)° (pyridine–pyridine). The single "wingtip" aromatic ring is nearly perpendicular to the rest of the ligand, with an interplane angle of 84.64(11)° between this and the imidazol-2-ylidene ring.

The imidazolium salt **6** has also been successfully used for the synthesis of the (carbene)silver complex **8** in good yields, by the reaction with Ag_2O in dichloromethane in

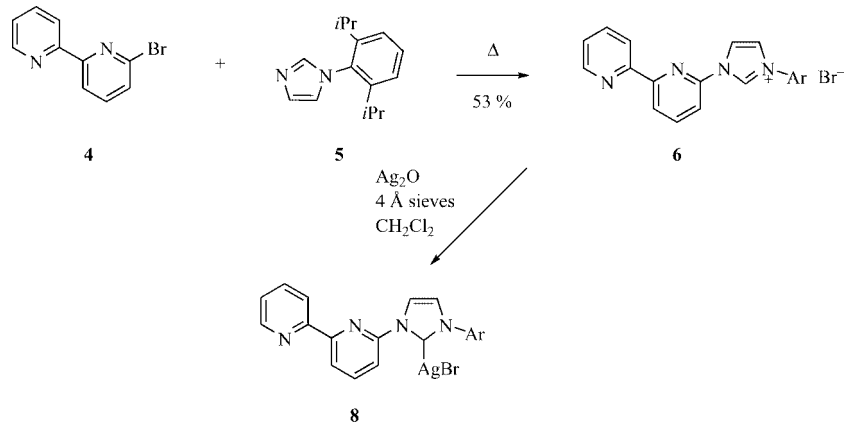

4 5 6 8

Scheme 3. Formation of the "bipy" salt **6** and attempt to deprotonate (Ar = 2,6-*i*Pr$_2$C$_6$H$_3$).

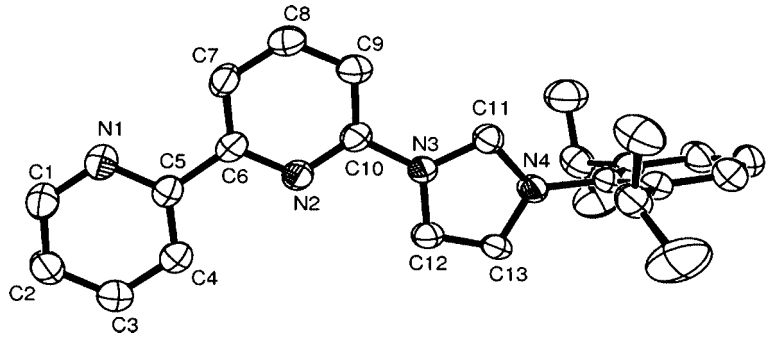

Figure 3. ORTEP representation of the structure of **7** showing 50% probability ellipsoids with hydrogen atoms omitted for clarity. Selected bond lengths [Å] and angles [°] with estimated standard deviations: C(11)–N(4) 1.361(3), C(11)–N(3) 1.375(3), C(5)–C(6) 1.486(4),C(10)–N(3) 1.427(3); N(4)–C(11)–N(3) 101.3(2).

the presence of molecular sieves (4 Å). The (carbene)silver complex was characterised by spectroscopic (NMR and MS) and analytical methods.

The Rh(C–N–N)X [X = Cl (**9b**), Br (**9a**)] complexes have been synthesised by two different routes on the basis of either the reaction of **6** with [(COD)Rh(OMe)]$_2$ (**9b**) or the reaction of **7** with [(COE)$_2$RhCl]$_2$ (**9a**) (Scheme 4).

The green, very air-sensitive complex was characterised by analytical and spectroscopic methods. Even though it is sparingly soluble in non-chlorinated solvents, meaningful ^{1}H NMR spectra of **9a** were recorded in [D$_8$]THF. The appearance of peaks assignable to the *i*Pr groups of the DiPP group supports the presence of a plane of symmetry in the molecule. However, the poor solubility of **9a** prevented the collection of strong ^{13}C{^{1}H} NMR spectroscopic data even after prolonged acquisition times. It is interesting to note that silver transmetallation reactions, which have been commonly used for the synthesis of NHC–Rh complexes were not successful here due to the reactivity of the initially formed Rh^I product with dichloromethane which is the

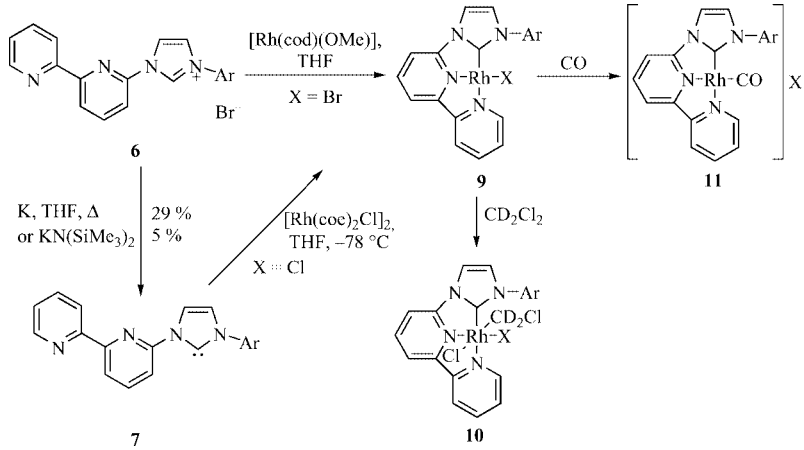

6 9 11 7 10

Scheme 4. Generation of free carbene **7** and complexes **9a** and **9b** (Ar = 2,6-*i*Pr$_2$C$_6$H$_3$; **9a**: X = Br; **9b**: X = Cl).

commonly used solvent in reactions of this type (vide infra). The structure of the complex was unequivocally established crystallographically (Figure 4).

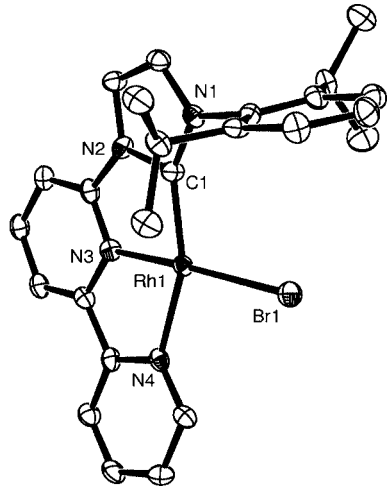

Figure 4. ORTEP representation of the structure of **9a** showing 50% probability ellipsoids with hydrogen atoms omitted for clarity. Selected bond lengths [Å] and angles [°] with estimated standard deviations: C(1)–Rh(1) 1.957(6), N(3)–Rh(1) 1.941(5), N(4)–Rh(1) 2.116(5), Br(1)–Rh(1) 2.4904(8); N(3)–Rh(1)–Br(1) 172.26(14), C(1)–Rh(1)–Br(1) 104.30(17), N(4)–Rh(1)–Br(1) 97.27(13).

The rhodium centre adopts a distorted square-planar geometry, with the rhodium atom being 0.034(2) Å out of the plane of the donor atoms. The terminal pyridine nitrogen atom N(4) is approx. 0.15 Å further from the metal centre than N(3). The Rh–C_{NHC} bonds [1.957(6) Å] are slightly shorter than those reported for **2**. In comparison to the recently reported blue Rh(terpy)Cl,[15] the corresponding Rh–$N_{pyridine}$ bonds in **9a** are longer.

Reactivity of 9a

The replacement in complex **2** of one NHC by the poorer σ-donating pyridine group to give **9** is expected to reduce the electron density on the metal atom. However, it should be more electron-rich than the metal atom in Rh(terpy)Cl.[15] In the latter, Rh^{I} has been classified as electron-rich on the basis of the oxidation potential of the complex, as measured by CV and DFT calculations. Complex **9a** reacts easily with dichloromethane at room temperature giving rise to the oxidative addition adduct **10** (Scheme 4), which was characterised by NMR spectroscopy in a way analogous to **3**. It also reacts fast with CO (1 bar, room temperature). The NMR spectra of the product suggest the formation of the CO adduct **11** (Scheme 4). The ^{1}H NMR spectrum of **11** shows a number of changes in the aromatic region, but significantly retains the single pair of doublets in the *i*Pr region: as before, this indicates retention of the plane of symmetry in the product. The CO adduct appears to be stable, and in contrast to **9a** it can be exposed to air and chlorinated solvents without degradation.

Attempts to carry out hydroformylation using **9** were not successful. Addition of CO/H_2 to a solution of the complex (0.2 mol-%) and styrene in toluene gave a rapid colour change to light orange. After 3 h at 70 °C under 9 bar of CO/H_2, analysis of the reaction mixture by GC-MS showed no hydroformylation products.

Theoretical Studies of Complexes 2 and 9b

In order to obtain a further insight into the bonding in the new (pincer)Rh^{I} complexes we performed DFT studies on **2** and **9b**. No symmetry restriction was imposed on the molecules. The Rh(C–N–C) and Rh(C–N–N) substructures in the calculated optimised geometries of **2-dft** and **9b-dft** are in very good agreement with those observed in the crystal structures (see Supporting Information). Only the bulky DiPP substituent is slightly dislocated, presumably due to crystal-packing effects.

The HOMO orbital of both complexes has d_{z^2} character. As expected, the LUMO of both **2-dft** and **9b-dft** reside on the π* system of the pyridine ligand, with some contribution of the metal atom. The HOMO–LUMO gap for **2-dft** of 2.92 eV is marginally larger than the gap for **9b-dft** (2.49 eV). For comparison, these values are much larger than the values reported for Rh(terpy)Cl (1.04 eV).[15] It is therefore plausible that this difference may lead to different reactivity of **2** and **9b** compared with Rh(terpy)Cl. This point is being investigated further in our laboratory.

For complex **2-dft**, the HOMO-1 has predominantly Cl(p_π)/Rh(d_{zx}) character, with some contribution of the pyridine ligand (see Supporting Information for plots of the orbitals). HOMO-2 is of similar character with some contribution from the NHC ligand to the Rh(d_{xy}) atom. HOMO-3 is predominantly on the metal atom [Rh(d_{yz})] and HOMO-4 is predominantly on the DiPP ligands and the chloride ion.

For complex **9b-dft**, similar observations can be made: HOMO-1 is predominately of Cl(p_π)/Rh(d_{zx}) character, with some contribution of the pyridine ligand *trans* to the chloride ion. HOMO-2 is of similar character as HOMO-2 of **2-dft**; however, the pyridine ligand *trans* to the NHC is less involved in the molecular orbital. HOMO-3 is again similar to HOMO-3 of **2-dft**; again the pyridine ligand *trans* to the NHC is not involved in the molecular orbital. HOMO-4 is predominately on the DiPP ligand.

The electronic environment in the complexes was further investigated by Natural Bonding Orbital (NBO) analysis. In **2-dft**, the lone pair of the pyridine nitrogen atom is donating into an empty orbital of the Rh atom. One of the NHC ligands is donating into an empty orbital of the Rh atom and into the antibonding orbital of the other Rh–C_{NHC} bond. However, unexpectedly, backdonation occurs from a filled d_{yz} orbital of the metal atom to antibonding orbitals of both the NHC and the pyridine ligand. For complex **9b-dft**, similar observations have been made. The lone pairs of the pyridine nitrogen atoms are donating into an empty d-orbital of the metal atom. The nitrogen atom *trans* to the NHC is donating into the carbene–metal antibonding orbital. A smaller contribution to this bonding is made by the

nitrogen atom on the other pyridine ligand. As with **2-dft**, a filled d-orbital of the metal atom is donating into an C–N antibonding orbital of the NHC. Backdonation from a different filled d-orbital of the metal atom to the pyridine ligand *trans* to the chloride ion is also observed. Orbital representation of the NBO analysis for both complexes are detailed in the Supporting Information.

As expected, the LUMO of both **2-dft** and **9b-dft** reside on the π* system of the pyridine ligand, with some contribution of the metal atom. The higher-lying virtual orbitals of **2-dft** and **9b-dft** are almost exclusively localised on the ligands. Exceptions are the LUMO+6 of **2-dft** and LUMO+5 of **9b-dft**, which are metal-based. Metal-based high-lying LUMOs have been observed before, notably for the complex Rh(terpy)Cl (LUMO+5).[15]

Conclusions

Highly reactive electron-rich Rh^{I} complexes with the pyridine-based dicarbene and bipyridyl-based monocarbene rigid tridentate pincers and without any π-acidic co-ligands have been prepared and characterised by spectroscopic and diffraction methods. The complexes easily undergo oxidative addition reactions of C–halide bonds, but are resistant to oxidative addition of other less polar bonds (H–H, Si–H, C–H, etc.). The Rh^{III} products obtained are extremely stable. The complexes also form stable adducts with the π-acidic CO, which are resistant to further reactions by alkenes, H_2, O_2, etc. The use of the new complexes as hydroformylation catalysts is hampered by rigid structures and stabilisation of the higher oxidation states by the strongly σ-donating ligand system. However, these "σ-loaded" rigid pincers may prove useful co-ligands in the stabilisation of higher oxidation states.

Experimental Section

General Methods: Solvents were dried by standard methods[16] and either used directly or stored in ampoules with molecular sieves (4 Å). All air- or moisture-sensitive reactions were carried out under dry nitrogen using standard Schlenk techniques or in an M. Braun glove box. NMR spectroscopic data were recorded with Bruker AMX-300 and DPX-400 spectrometers, operating at 300 and 400 MHz (^{1}H), respectively. The spectra were referenced internally using the signal from the residual protio solvent (^{1}H) or the signals of the solvent (^{13}C). Mass spectra (electrospray ionisation) were obtained from acetonitrile solutions with a VG Biotec platform. The calculated isotopic envelopes agree well with the experimentally observed patterns. Commercial chemicals were from Acros, Aldrich, Lancaster and Avocado; the light petroleum ether had boiling range of 40–60 °C. The following starting materials were prepared as described in the literature: 3,3′-Bis(2,6-diisopropylphenyl)-1,1′-pyridine-2,6-diylbis(imidazol-3-ium) dibromide,[5b] 6-bromo-2,2′-bipyridine,[11,12] 3-(2,6-diisopropylphenyl)-1*H*-imidazole,[17] bis[μ-chlorobis(η^2-cyclooctene)rhodium(I)],[18] bis[μ-chlorobis(η^2-ethene)rhodium(I)][19] and bis[μ-methoxybis(η^2-cyclooctene)rhodium(I)].[20]

3,3′-Bis(2,6-diisopropylphenyl)-1,1′-pyridine-2,6-diylbis(imidazol-2-ylidene) (1): The synthesis was carried out by an improved version of the previously published procedure.[5b] Thus, the corresponding bis(imidazolium) salt (CH–N–CH)Br_2 (Ar = 2,6-*i*$Pr_2C_6H_3$) (6.89 g, 9.93 mmol) was suspended in THF (100 mL) in a large Schlenk tube, and cooled to –78 °C. A solution of potassium bis(trimethylsilyl)amide (4.32 g, 21.6 mmol) in THF (100 mL) was cooled to –78 °C and added to the salt suspension. The reaction mixture was warmed to room temperature overnight, the solvent evaporated and the residue dissolved in toluene (100 mL). The dark-brown solution was filtered through a pad of Celite®, and the volume reduced to ca. 20 mL. Dilution with petroleum ether (40 mL) led to the precipitation of the product, which was filtered off, washed with petroleum ether and dried under vacuum to yield a cream-colored solid (4.09 g, 77%). ^{1}H NMR (300 MHz, C_6D_6, 25 °C): δ = 1.20 (d, J = 6.9 Hz, 12 H, Me), 1.29 (d, J = 6.8 Hz, 6 H, Me), 3.01 [sept, J = 6.9 Hz, 4 H, *C*H(CH$_3$)$_2$], 6.73 (d, J = 1.7 Hz, 1 H, imidazole backbone), 7.16 (t, J = 8.0 Hz, 1 H, central CH of pyridine), 7.25 (d, J = 7.5 Hz, 4 H, aromatic CH), 7.35 (d, J = 6.9 Hz, 1 H, aromatic CH), 7.38 (d, J = 6.9 Hz, 1 H, aromatic CH), 8.17 (d, J = 1.7 Hz, 2 H, imidazole backbone), 8.54 (d, J = 8.0 Hz, 2 H, outer 2×CH of pyridine) ppm. ^{13}C NMR (75.45 MHz, C_6D_6, 25 °C): δ = 24.0 (Me), 24.4 (Me), 28.6 [*C*H(CH$_3$)$_2$], 111.7 (aromatic CH), 116.3 (aromatic CH), 122.8 (aromatic CH), 123.8 (aromatic CH), 129.3 (aromatic CH), 138.7 (aromatic C), 140.7 (aromatic C), 146.2 (aromatic CH), 152.6 (aromatic C), 220.4 (carbene) ppm.

3,3′-Dimesityl-1,1′-pyridine-2,6-diylbis(imidazol-2-ylidene) (1b): This was prepared according to a similar route to **1** from the salt (CH–N–CH)Br_2 (Ar = mesityl) (2.78 g, 4.00 mmol) and potassium bis(trimethylsilyl)amide (1.68 g, 8.42 mmol). After the reaction, the crude solid was dissolved in benzene (60 mL) and worked up as for **1**. This gave the product as a cream-colored solid (1.07 g, 60%). ^{1}H NMR (300 MHz, C_6D_6, 25 °C): δ = 2.12 (s, 12 H, Me), 2.14 (s, 6 H, Me), 6.44 (d, J = 1.4 Hz, 2 H, imidazole backbone), 6.79 (s, 4 H, aromatic CH), 7.09 (t, J = 7.6 Hz, 1 H, central CH of pyridine), 8.11 (d, J = 1.4 Hz, 2 H, imidazole backbone), 8.54 (d, J = 7.6 Hz, 2 H, outer 2×CH of pyridine) ppm. ^{13}C (75.45 MHz, C_6D_6, 25 °C): δ = 18.1 (Me), 21.0 (Me), 111.5 (aromatic CH), 116.5 (aromatic CH), 119.7 (aromatic CH), 129.0 (aromatic C), 129.2 (aromatic C), 130.4 (aromatic CH), 135.3 (aromatic C), 138.9 (aromatic C), 140.7 (aromatic CH), 152.69 (carbene) ppm.

[3,3′-Bis(2,6-diisopropylphenyl)-1,1′-pyridine-2,6-diylbis(imidazol-2-ylidene)]chlororhodium(I) (2): A solution of carbene **1** (162 mg, 0.305 mmol) in THF (10 mL) was added to a suspension of bis[μ-chlorobis(η^2-ethene)rhodium(I)] (60 mg, 0.154 mg) in THF (5 mL), leading to an immediate colour change to dark purple. The solution was stirred under an oil bubbler for 90 min, before evaporation of the solvent. The residue was washed with petroleum ether (2×5 mL) to leave a dark purple solid (124 mg, 61%). Layering of a THF solution of this residue with an equal volume of petroleum ether led to the formation of X-ray quality crystals. ^{1}H NMR (300 MHz, C_6D_6, 25 °C): δ = 1.14 (d, J = 7.0 Hz, 12 H, Me), 1.44 (d, J = 6.8 Hz, 12 H, Me), 3.06 [sept, J = 6.9 Hz, 4 H, C*H*(CH$_3$)$_2$], 6.08 (d, J = 8.1 Hz, 2 H, pyridyl CH), 6.42 (d, J = 2.0 Hz, 2 H, imidazole backbone), 6.83 (d, J = 2.0 Hz, 2 H, imidazole backbone), 7.19 (d, J = 7.3 Hz, 4 H, aromatic CH), 7.33 (t, J = 7.3 Hz, 2 H, aromatic CH), 7.45 (t, J = 8.1 Hz, 1 H, pyridyl CH) ppm. ^{13}C NMR (75.45 MHz, [D$_8$]THF, 25 °C): δ = 24.3 (Me), 24.5 (Me), 29.3 (Me), 104.8 (aromatic CH), 114.3 (aromatic CH), 123.7 (aromatic CH), 125.6 (aromatic CH), 126.8 (aromatic CH), 129.4 (aromatic CH), 137.3 (aromatic C), 146.3 (aromatic C), 152.7 (aromatic C) ppm; carbene signal not observed. $C_{35}H_{41}ClN_5Rh$ (670.10): calcd. C 62.73, H 6.17, N 10.45; found C 62.65, H 6.05, N 10.25.

3,3′-Bis(2,6-diisopropylphenyl)-1,1′-pyridine-2,6-diylbis(imidazol-2-ylidene)dichloro(chloromethyl)rhodium(III) (3): Dissolution of the

rhodium(I) complex **2** (ca. 15 mg) in CD_2Cl_2 (0.75 mL) led to a rapid colour change from purple to light yellow. Upon standing, light yellow crystals suitable for X-ray diffraction formed in quantitative yield. ^{1}H NMR (300 MHz, CD_2Cl_2, 25 °C): δ = 0.96 (d, J = 7.0 Hz, 6 H, Me), 1.11 (d, J = 6.8 Hz, 6 H, Me), 1.15 (d, J = 6.8 Hz, 6 H, Me), 1.21 (d, J = 6.5 Hz, 6 H, Me), 2.55 [sept, J = 6.7 Hz, 2 H, C*H*$(CH_3)_2$], 3.36 [sept, J = 6.7 Hz, 2 H, C*H*$(CH_3)_2$], 7.07 (d, J = 2.4 Hz, 2 H, imidazole backbone), 7.15 (d, J = 7.6 Hz, 2 H, aromatic CH), 7.19 (d, J = 8.1 Hz, 2 H, aromatic CH), 7.35 (t, J = 7.6 Hz, 2 H, aromatic CH), 7.49 (dm, J = 8.1 Hz, 2 H, pyridyl CH), 7.85 (d, J = 2.4 Hz, 2 H, imidazole backbone), 8.12 (t, J = 8.1 Hz, 1 H, pyridyl CH) ppm. ^{13}C (75.45 MHz, CD_2Cl_2, 25 °C): δ = 22.9 (Me), 23.0 (Me), 26.0 (Me), 26.3 (Me), 28.4 [*C*H$(CH_3)_2$], 28.5 [C*H*$(CH_3)_2$], 68.1 (CD_2Cl) 106.1 (aromatic CH), 116.2 (aromatic CH), 123.3 (aromatic CH), 124.2 (aromatic CH), 126.3 (aromatic CH), 130.1 (aromatic CH), 134.4 (aromatic C), 141.3 (aromatic C), 145.2 (aromatic CH), 147.8 (aromatic C), 162.8 (aromatic C) ppm, carbene not observed.

1-(2,2′-Bipyridin-6-yl)-3-(2,6-diisopropylphenyl)-3*H*-imidazol-1-ium Bromide (6): 6-Bromo-2,2′-bipyridine (1.40 g, 5.95 mmol) and 1-(2,6-diisopropylphenyl)imidazole (1.46 g, 6.38 mmol) were placed in a glass ampoule which was sealed under vacuum. This was completely immersed in an oil bath at 150 °C for 6 d. After cooling to room temperature, the ampoule was opened and the brown residue was dissolved in dichloromethane. After evaporation of the solvent, the product was stirred with diethyl ether at 0 °C for several hours, the solvent removed by filtration and the solid dried in vacuo. This gave the product as a brown solid (2.27 g, 82%). $C_{25}H_{27}BrN_4$ (463.42): calcd. C 64.79, H 5.87, N 12.09; found C 64.31, H 5.98, N 11.92. ^{1}H NMR (300 MHz, $CDCl_3$, 25 °C): δ = 1.19 (d, J = 6.6 Hz, 6 H, Me), 1.32 (d, J = 6.6 Hz, 6 H, Me), 2.46 [sept, J = 6.6 Hz, 2 H, C*H*$(CH_3)_2$], 7.37 (d, J = 7.5 Hz, 2 H, aromatic CH), 7.42 (br. s, 1 H, pyridyl CH), 7.59 (t, J = 7.9 Hz, 1 H, aromatic CH), 7.68 (br. s, 1 H, pyridyl CH), 8.25 (t, J = 7.9 Hz, 2 H, pyridyl CH), 8.62–8.75 (m, 3 H, pyridyl CH), 9.33 (d, J = 7.9 Hz, 1 H, pyridyl CH), 9.37 (br. s, 1 H, imidazole backbone), 11.30 (s, 1 H, imidazolium salt) ppm. ^{13}C NMR (74.45 MHz, $CDCl_3$, 25 °C): δ = 24.0 (Me), 24.1 (Me), 28.6 [*C*H$(CH_3)_2$], 116.9 (aromatic CH), 121.2 (aromatic CH), 123.5 (aromatic CH), 124.5 (aromatic CH), 125.5 (aromatic CH), 125.6 (aromatic CH), 129.8 (aromatic C), 131.9 (aromatic CH), 136.2 (aromatic CH), 142.2 (aromatic CH), 144.8 (aromatic C), 145.6 (aromatic C) ppm. MS (ESI+): m/z = 155.0, 367.3, 170.0, 182.1, 196.1, 213.1, 352.2, 383.3 [M^+].

1-(2,2′-Bipyridin-6-yl)-3-(2,6-diisopropylphenyl)imidazol-2-ylidene (7): The salt **6** (1.02 g, 2.21 mmol) and potassium bis(trimethylsilyl)amide (0.56 g, 2.81 mmol) were stirred under nitrogen and cooled to –78 °C. Pre-cooled THF (35 mL) was added, and the solution stirred at low temperature for 1 h. It was warmed to –30 °C, then left to stand overnight. After evaporation of the solvent, the product was filtered through Celite® as a solution in toluene (20 mL). Reduction to a volume of 2 mL was followed by addition of petroleum ether (10 mL); cooling to –30 °C gave the product as a brown solid (36 mg, 4%). Better yields are obtained as follows: Potassium metal (348 mg, 8.9 mmol) was added to **6** (3.00 g, 5.25 mmol) in THF (120 mL) and the mixture heated to reflux overnight. After cooling to room temperature, the solution was filtered through Celite® and the solvent removed in vacuo. The solid residue was dissolved in toluene (70 mL), the solution filtered and the volume reduced to ca. 15 mL. After addition of petroleum ether (50 mL), the product was crystallised at –30 °C. Filtration and washing with petroleum ether (20 mL) gave the carbene as a brown solid (586 mg, 29%). ^{1}H NMR (300 MHz, C_6D_6, 25 °C): δ = 1.13 (d, J = 6.9 Hz, 6 H, Me), 1.22 (d, J = 6.8 Hz, 6 H, Me), 2.94 [sept, J = 6.9 Hz, 2 H, C*H*$(CH_3)_2$], 6.66 (d, J = 1.6 Hz, 1 H, imidazole backbone CH), 6.74 (ddd, J = 1.1, 4.7, 7.4 Hz, 1 H, aromatic CH), 7.19–7.32 (m, 5 H, aromatic CH), 8.28 (d, J = 1.7 Hz, 1 H, imidazole backbone CH), 8.48–8.56 (m, 3 H, aromatic CH), 8.66 (d, J = 8.2 Hz, 1 H, aromatic CH) ppm. ^{13}C NMR (75.45 MHz, C_6D_6, 25 °C): δ = 22.82 (Me), 23.17 (Me), 27.36 [*C*H$(CH_3)_2$], 113.80 (aromatic CH), 115.13 (aromatic CH), 117.63 (aromatic CH), 119.61 (aromatic CH), 121.56 (aromatic CH), 122.55 (aromatic CH), 127.07 (aromatic CH), 127.98 (aromatic CH), 135.19 (aromatic CH), 138.07 (aromatic CH), 145.01 (aromatic C), 148.27 (aromatic CH), 152.34 (aromatic C), 153.46 (aromatic C), 154.98 (aromatic C) ppm; carbene carbon signal not observed. X-ray quality colourless crystals were obtained by cooling solutions of **7** in toluene/petroleum ether (50:50) at –30 °C.

[1-(2,2′-Bipyridin-6-yl)-3-(2,6-diisopropylphenyl)imidazol-2-ylidene]-silver(I) Bromide (8): The imidazolium salt **6** (1.00 g, 2.16 mmol), molecular sieves (4 Å) (ca. 5 g) and Ag_2O were suspended in the dark in CH_2Cl_2 (30 mL) and the mixture refluxed overnight. After cooling to room temperature, the solution was filtered through Celite® and the solvent removed in vacuo. The product was obtained as a pale brown solid (881 mg, 71%). $C_{25}H_{26}AgBrN_4$ (570.3): calcd. C 52.65, H 4.59, N 9.82; found C 52.15, H 4.44, N 9.68. ^{1}H NMR (300 MHz, $CDCl_3$, 25 °C): δ = 1.21 (d, J = 6.6 Hz, 6 H, Me), 1.34 (d, J = 6.6 Hz, 6 H, Me), 2.57 [sept, J = 6.6 Hz, 2 H, C*H*$(CH_3)_2$], 7.24 (br. s, 1 H, imidazole backbone CH), 7.36 (d, J = 8.0 Hz, 2 H, aromatic CH), 7.43 (m, 1 H, aromatic CH), 7.54 (t, J = 8.0 Hz, 1 H, central aromatic CH), 8.12 (t, J = 7.4 Hz, 1 H, aromatic CH), 8.26 (br. s, 1 H, imidazole backbone CH), 8.30 (d, J = 8.1 Hz, 2 H, aromatic CH), 8.61 (m, 2 H, aromatic CH), 8.78 (br. s, 1 H, aromatic CH) ppm. ^{13}C NMR (75.45 MHz, $CDCl_3$, 25 °C): δ = 24.40 (Me), 24.50 (Me), 28.40 [*C*H$(CH_3)_2$], 115.07 (aromatic CH), 119.94 (aromatic CH), 121.18 (aromatic CH), 124.38 (aromatic CH), 124.50 (aromatic CH), 128.18 (aromatic C), 128.90 (aromatic C), 130.75 (aromatic CH), 140.36 (aromatic CH), 145.52 (aromatic C), 149.36 (aromatic CH), 172.20 (s, carbene) ppm. MS (ES^+): m/z = 871.5 [carbene$_2$$Ag^+$].

[1-(2,2′-Bipyridin-6-yl)-3-(2,6-diisopropylphenyl)imidazol-2-ylidene]-rhodium(I) Halide [Halide = Br (9a), Cl (9b)]: The salt **6** (93 mg, 0.20 mmol) was suspended in THF (5 mL) and cooled to –78 °C, and a solution of bis[μ-methoxybis(η^2-cyclooctene)rhodium(I)] (49 mg, 0.10 mmol) in THF (5 mL) at –78 °C was added. The solution was warmed to room temperature and became red, then brown and finally dark green. A small amount of solid was filtered off, and the solution diluted with petroleum ether (15 mL). The resulting precipitate was filtered off, dissolved in THF (5 mL) and layered with petroleum ether (5 mL). Cooling to –30 °C gave green crystals of the title compound suitable for X-ray diffraction. $C_{25}H_{26}BrN_4Rh$ (565.32): calcd. C 53.12, H 4.64, N 9.91; found C 52.78, H 4.42, N 9.73. ^{1}H NMR ([D$_8$]THF): δ = 1.13 (d, J = 6.9 Hz, 6 H, Me), 1.21 (d, J = 6.8 Hz, 6 H, Me), 3.00 [sept, J = 6.9 Hz, 2 H, C*H*$(CH_3)_2$], 7.20 (m, 3 H, aromatic CH), 7.35 (t, J = 8.2 Hz, 1 H, aromatic CH), 7.44 (d, J = 8.0 Hz, 1 H, aromatic CH), 7.71 (d, J = 8.0 Hz, 1 H, aromatic CH), 7.76 ("t", J = 6.0 Hz, 1 H, aromatic CH), 8.10 (m, 2 H, aromatic CH), 8.21 (d, J = 8.0 Hz, 1 H, aromatic CH), 8.26 (t, J = 8.0 Hz, 1 H, aromatic CH), 9.47 (d, 1 H, imidazole backbone CH) ppm. The chloride analogue **9b** can be obtained as green powder by the reaction of **7** generated in situ with $[Rh(COE)_2Cl]_2$ in THF at room temperature for 2 h. It exhibits identical NMR spectroscopic data to **9a**. $C_{25}H_{26}ClN_4Rh$ (520.9): calcd. C 57.65, H 5.03, N 10.76; found C 57.12, H 4.87, N 10.61.

Oxidative Addition Adduct 10 of 9a with CD_2Cl_2: Addition of CD_2Cl_2 to a solid sample of **9a** initially gave a dark green solution,

but this rapidly became brown (ca. 5 min.). The product of this reaction was the oxidative addition complex **10**. Yield quantitative. ^{1}H NMR (300 MHz, CD_2Cl_2, 25 °C): δ = 1.05 (d, J = 6.9 Hz, 3 H, Me), 1.17 (d, J = 6.8 Hz, 3 H, Me), 1.30 (d, J = 6.8 Hz, 3 H, Me), 1.35 (d, J = 6.8 Hz, 3 H, Me), 2.66 [sept, J = 6.8 Hz, 1 H, C*H*-$(CH_3)_2$], 3.47 [sept, J = 6.6 Hz, 1 H, C*H*$(CH_3)_2$], 7.08 (d, J = 2.2 Hz, 1 H, imidazole backbone CH), 7.33 (ddd, J = 1.1, 7.7, 14.3 Hz, 2 H, 2 aromatic CH), 7.52 (t, J = 7.8 Hz, 1 H, aromatic CH), 7.64 (m, 1 H, aromatic CH), 7.63 (t, J = 6.5 Hz, 1 H, aromatic CH), 7.76 (d, J = 8.1 Hz, 1 H, aromatic CH), 8.00 (m, 2 H, aromatic CH), 8.05 (dd, J = 1.3, 7.8 Hz, 1 H, aromatic CH), 8.11 (t, J = 8.1 Hz, 1 H, aromatic CH), 8.19 (d, J = 7.9 Hz, 1 H, aromatic CH), 9.14 (d, J = 4.8 Hz, 1 H, aromatic CH) ppm. ^{13}C NMR (75.45 MHz, CD_2Cl_2, 25 °C): δ = 23.28 (Me), 23.59 (Me), 26.28 (Me), 26.80 (Me), 28.92 [*C*H$(CH_3)_2$], 28.99 [*C*H$(CH_3)_2$], 112.05 (aromatic CH), 117.37 (aromatic CH), 119.17 (aromatic CH), 123.92 (aromatic CH), 124.12 (aromatic CH), 124.85 (aromatic CH), 126.71 (aromatic CH), 128.31 (aromatic CH), 131.01 (aromatic CH), 134.94 (aromatic C), 139.47 (aromatic CH), 140.60 (aromatic CH), 146.01 (aromatic C), 148.25 (aromatic C), 150.90 (aromatic C), 152.04 (aromatic C), 155.90 (aromatic C) ppm; carbene and CD_2Cl signals not observed. MS (ESI+): m/z = 570.9 [M^+ – HCl], 611.9 [M^+ – HCl + MeCN].

Reaction of 9a with CO: To a green solution of **9a** in THF was bubbled CO for 1 min. The colour changed to dark red-orange within 5 min and a pink precipitate appeared after sometime which was isolated by filtration and dried. Yield: 45%. ^{1}H NMR (300 MHz, CD_2Cl_2, 25 °C): δ = 1.05 (d, J = 6.9 Hz, 3 H, Me), 1.17 (d, J = 6.8 Hz, 3 H, Me), 1.30 (d, J = 6.8 Hz, 3 H, Me), 1.35 (d, J = 6.8 Hz, 3 H, Me) 2.66 [sept, J = 6.8 Hz, 1 H, C*H*$(CH_3)_2$], 3.47 [sept, J = 6.8 Hz, 1 H, C*H*$(CH_3)_2$], 7.33 (ddd, J = 1.1, 7.7, 14.3 Hz, 2 H, aromatic), 7.52 (t, J = 7.8 Hz, 1 H, aromatic), 7.63 (t, J = 6.5 Hz, 1 H, aromatic), 7.76 (d, J = 8.1 Hz, 1 H, aromatic), 8.00 (m, 2 H, aromatic), 8.05 (dd, J = 1.3, 7.8 Hz, 1 H, aromatic), 8.11 (t, J = 8.1 Hz, 1 H, aromatic), 8.19 (d, J = 7.9 Hz, 1 H, aromatic) 9.14 (d, J = 4.8 Hz, 1 H, aromatic) ppm. ^{13}C NMR (75.45 MHz, CD_2Cl_2, 25 °C): δ = 23.80 (Me), 24.45 (Me), 28.47 [*C*H$(CH_3)_2$], 114.46 (aromatic CH), 118.79 (aromatic CH), 120.58 (aromatic CH), 124.08 (aromatic CH), 124.35 (aromatic CH), 124.41 (aromatic CH), 128.01 (aromatic CH), 130.99 (aromatic CH), 134.18 (aromatic C), 140.53 (aromatic CH), 144.77 (aromatic CH), 145.66 (aromatic C), 152.24 (aromatic C), 154.29 (aromatic CH), 154.97 (aromatic C), 156.09 (aromatic C) ppm.

X-ray Crystallography: A summary of the crystal data, data collection and refinement for compounds **2**, **3**, **7**, and **9a** are given in Table 1. All data sets were collected with an Enraf–Nonius Kappa CCD area detector diffractometer, fitted with an FR591 rotating anode (Mo-K_α radiation) and an Oxford Cryosystems low-temperature device, operating in ω-scanning mode with ψ- and ω-scans to fill the Ewald sphere. Data collection and reduction were carried out using the software packages Collect, Scalepack, and Denzo.[21] The crystals were mounted on a glass fibre with silicon grease from Fomblin vacuo oil. In all cases refinement was carried out by full-matrix least-squares methods using SHELXL-97[22] within the WinGX program suite.[23] All non-hydrogen atoms were refined using anisotropic thermal parameters, and hydrogen atoms were added using a riding model. CCDC-607971 (**2**), -607972 (**3**), -607973 (**7**) and -607974 (**9a**) contain the supplementary crystallographic data for this paper. These data can be obtained free of charge from The Cambridge Crystallographic Data Centre via www.ccdc.cam.ac.uk/data_request/cif.

Computational Details: DFT calculations were carried out using the GAUSSIAN03[24] program package, running on a Mandriva Linux Dual-Opteron. Geometries have been fully optimised without symmetry constraints, involving the functional combinations according to Becke[25] (hybrid) and Lee, Yang, Parr[26] (denoted B3LYP), with the corresponding valence basis set for Rh (Stuttgart-Dresden, keyword SDD in Gaussian) and standard 6-31G* basis set for C, H, N and Cl (denoted as ECP1).[27] The stationary points were characterised as minima by analytical harmonic frequency (zero imaginary frequency), which were used without scaling for zero-point and thermal corrections. MOLDEN[28] was used for the chemical representation of the calculated compounds, and NBO-View[29] for the representation of the orbitals. Tables of Cartesian coordinates of all calculated structures are available as Supporting Information in x, y, z format.

Table 1. Summary of crystallographic data for **2**, **3**, **7**, and **9a**.

	2	**3**	**7**	**9a**
Empirical formula	$C_{35}H_{41}ClN_5Rh$	$C_{36}H_{43}Cl_3N_5Rh{\cdot}CH_2Cl_2$	$C_{25}H_{26}N_4$	$C_{25}H_{26}BrN_4Rh$
Formula mass	670.09	839.94	382.50	565.32
Crystal description	purple block	light yellow prism	orange prism	dark green plate
Crystal dimensions [mm]	0.10×0.17×0.20	0.06×0.06×0.20	0.12×0.12×0.18	0.02×0.06×0.10
Crystal system	tetragonal	monoclinic	monoclinic	triclinic
Space group	$P\bar{4}2_1c$	$P2_1/c$	$P2_1/n$	$P\bar{1}$
a [Å]	20.1073(9)	11.2296(2)	8.5183(11)	7.9185(12)
b [Å]	20.1073(9)	18.5984(5)	10.7315(11)	8.5368(12)
c [Å]	16.5070(12)	18.2031(5)	23.237(3)	17.452(3)
α [°]	90	90	90	86.492(5)
β [°]	90	95.905(2)	92.215(5)	79.947(4)
γ [°]	90	90	90	72.753(4)
V [Å^3]	6673.8(6)	3781.59(16)	2122.6(4)	1109.3(3)
Z	8	4	4	2
T [K]	120(2)	120(2)	120(2)	120(2)
μ [mm^{-1}]	0.623	0.839	0.072	2.591
No. of data collected	19201	24805	13277	15065
No. of unique data	6775	3812	4754	4870
R_{int}	0.0901	0.0883	0.0914	0.1160
R_1 [$I>2\sigma(I)$]	0.0935	0.0399	0.0856	0.0618
wR_2 (all data)	0.1979	0.0979	0.1730	0.1470

Supporting Information (see footnote on the first page of this article): Tables of cartesian coordinates (*x*, *y*, *z* format) of all calculated structures, HOMO/LUMO and selected NBO graphical respresentations.

Acknowledgments

We thank ICI Plc (Quest International) for generous support and Professor M. B. Hursthouse for the provision of X-ray facilities.

[1] A. Arduengo, R. L. Harlow, M. Kline, *J. Am. Chem. Soc.* **1991**, *113*, 361–363.
[2] a) W. A. Herrmann, *Angew. Chem. Int. Ed.* **2002**, *41*, 1290–1309; b) D. S. Clyne, J. Jin, E. Genest, J. C. Gallucci, T. V. RajanBabu, *Org. Lett.* **2000**, *2*, 1125–1128 (binaphthyl-substituted NHCs); c) B. Bildstein, M. Malaun, G. Opromolla, P. Zanello, *Organometallics* **1999**, *18*, 4325–4336 (ferrocenyl-substituted NHCs); d) J. C. Garrison, R. S. Simons, J. M. Talley, C. Wesdemiotis, C. A. Tessier, W. J. Youngs, *Organometallics* **2001**, *20*, 1276–1278; e) M. V. Baker, B. W. Skelton, A. White, C. C. Williams, *J. Chem. Soc., Dalton Trans.* **2001**, 111–120 (cyclophane-substituted NHCs).
[3] M. Albrecht, G. van Koten, *Angew. Chem. Int. Ed.* **2001**, *40*, 3750–3781, and references therein.
[4] For recent selected references, see: a) M. Gerisch, J. R. Krumper, R. G. Bergman, T. D. Tilley, *J. Am. Chem. Soc.* **2001**, *123*, 5818–5819; b) F. Guerin, D. H. McConville, J. J. Vittal, *Organometallics* **1996**, *15*, 5586–5590; c) B. L. Small, M. Brookhart, A. M. Bennett, *J. Am. Chem. Soc.* **1998**, *120*, 404–4050; d) G. J. P. Britovsek, V. C. Gibson, B. S. Kimberley, P. J. Maddox, S. J. McTavish, G. A. Solan, A. J. P. White, D. J. Williams, *Chem. Commun.* **1998**, 849–850; e) M. Gandelman, B. Rybtchinski, N. Ashkenazi, R. M. Gauvin, D. Milstein, *J. Am. Chem. Soc.* **2001**, *123*, 5372–5373.
[5] a) A. A. Danopoulos, S. Winston, W. B. Motherwell, *Chem. Commun.* **2002**, 1376–1377; b) A. A. Danopoulos, A. A. D. Tulloch, S. Winston, G. Eastham, M. B. Hursthouse, *Dalton Trans.* **2003**, 1009–1015; c) A. A. Danopoulos, N. Tsoureas, J. A. Wright, M. E. Light, *Organometallics* **2004**, *23*, 166–168; d) A. A. Danopoulos, J. A. Wright, W. B. Motherwell, S. Ellwood, *Organometallics* **2004**, *23*, 4807–4810; e) A. A. Danopoulos, J. A. Wright, W. B. Motherwell, *Chem. Commun.* **2005**, 784–786.
[6] J. M. Wilson, G. J. Sunley, H. Adams, A. Haynes, *J. Organomet. Chem.* **2005**, *690*, 6089–6095.
[7] M. Poyatos, E. Mas-Marzá, J. A. Mata, M. Sanaú, E. Peris, *Eur. J. Inorg. Chem.* **2003**, 1215–1221.
[8] a) P. N. W. M. van Leeuwen, C. Claver, *Rhodium Catalysed Hydroformylation*, Kluwer, Dordrecht, **2000**; b) C. D. Frohling, C. W. Kohlpaintner, in *Applied Homogeneous Catalysis with Organometallic Compound*s (Eds.: B. Cornils, W. A. Herrmann), VCH, Weinheim, **1996**, vol. 1, pp. 27–104.
[9] G. Vassapolo, P. Giannocarro, C. F. Nobile, A. Sacco, *Inorg. Chim. Acta* **1981**, *48*, 125–128.
[10] E. Poverenov, G. Leitus, J. W. Shimon, D. Milstein, *Organometallics* **2005**, *24*, 5937–5944.
[11] T. Norrby, A. Börje, L. Zhang, B. Åkermark, *Acta Chem. Scand.* **1998**, *52*, 77–85.
[12] J. S. Field, R. J. Haines, C. J. Perry, S. H. Sookraj, *S. Afr. J. Chem.* **1993**, *46*, 70–74.
[13] B. Gorodetsky, T. Ramnial, N. R. Branda, J. A. C. Clyburne, *Chem. Commun.* **2004**, 1972–1973.
[14] A. A. Danopoulos, S. Winston, W. B. Motherwell, *Chem. Commun.* **2002**, 1376–1377.
[15] B. C. de Pater, H.-W. Frühauf, K. Vrieze, R. de Gelder, E. J. Baerends, D. McCormack, M. Lutz, A. L. Spek, F. Hartl, *Eur. J. Inorg. Chem.* **2004**, 1675–1686.
[16] W. L. F. Armarego, D. D. Perrin, *Purification of Laboratory Chemicals*, 4th ed., Butterworth-Heinemann, Oxford, **1996**.
[17] A. L. Johnson, *US Patent* **1972**, 3637731.
[18] A. van der Ent, A. L. Onderdelinden, *Inorg. Synth.* **1990**, *28*, 90–92.
[19] R. Cramer, *Inorg. Synth.* **1990**, *28*, 86–88.
[20] R. Uson, L. A. Oro, J. A. Cabeza, *Inorg. Synth.* **1985**, *23*, 126–130.
[21] a) R. W. W. Hooft, COLLECT data collection software, Nonius B. V., **1998**; b) SCALEPACK, DENZO: Z. Otwinoski, W. Minor, *Methods Enzymol.* **1997**, *276*, 307–326.
[22] G. M. Sheldrick, *Programs for Crystal Structure Analysis*, University of Göttingen, Germany, **1997**.
[23] L. J. Farrugia, *J. Appl. Crystallogr.* **1999**, *32*, 837–838.
[24] M. J. Frisch, G. W. Trucks, H. B. Schlegel, G. E. Scuseria, M. A. Robb, J. R. Cheeseman, J. A. Montgomery Jr, T. Vreven, K. N. Kudin, J. C. Burant, J. M. Millam, S. S. Iyengar, J. Tomasi, V. Barone, B. Mennucci, M. Cossi, G. Scalmani, N. Rega, G. A. Petersson, H. Nakatsuji, M. Hada, M. Ehara, K. Toyota, R. Fukuda, J. Hasegawa, M. Ishida, T. Nakajima, Y. Honda, O. Kitao, H. Nakai, M. Klene, X. Li, J. E. Knox, H. P. Hratchian, J. B. Cross, V. Bakken, C. Adamo, J. Jaramillo, R. Gomperts, R. E. Stratmann, O. Yazyev, A. J. Austin, R. Cammi, C. Pomelli, J. W. Ochterski, P. Y. Ayala, K. Morokuma, G. A. Voth, P. Salvador, J. J. Dannenberg, V. G. Zakrzewski, S. Dapprich, A. D. Daniels, M. C. Strain, O. Farkas, D. K. Malick, A. D. Rabuck, K. Raghavachari, J. B. Foresman, J. V. Ortiz, Q. Cui, A. G. Baboul, S. Clifford, J. Cioslowski, B. B. Stefanov, G. Liu, A. Liashenko, P. Piskorz, I. Komaromi, R. L. Martin, D. J. Fox, T. Keith, M. A. Al-Laham, C. Y. Peng, A. Nanayakkara, M. Challacombe, P. M. W. Gill, B. Johnson, W. Chen, M. W. Wong, C. Gonzalez, J. A. Pople, *Gaussian03*, Gaussian, Inc., Pittsburgh, PA, **2004**.
[25] A. D. Becke, *J. Chem. Phys.* **1993**, *98*, 5648–5652.
[26] C. Lee, W. Yang, R. G. Parr, *Phys. Rev. B* **1988**, *37*, 785–789.
[27] W. J. Hehre, R. Ditchfield, J. A. Pople, *J. Chem. Phys.* **1972**, *56*, 2257–2261.
[28] G. Schaftenaar, J. H. Noordik, *J. Comput.-Aided Mol. Des.* **2000**, *14*, 123–134.
[29] E. D. Glendening, J. K. Badenhoop, A. E. Reed, J. E. Carpenter, J. A. Bohmann, C. M. Morales, F. Weinhold, *NBO 5.G.*, Theoretical Chemistry Institute, University of Wisconsin, Madison, USA, **2001**.

Received: June 16, 2006
Published Online: October 5, 2006

